Nanoplasmonic optical switch based on Ga-Si₃N₄-Ga waveguide

Wangshi Zhao
Zhaolin Lu

Nanoplasmonic optical switch based on Ga-Si$_3$N$_4$-Ga waveguide

Wangshi Zhao
Zhaolin Lu
Rochester Institute of Technology
Kate Gleason College of Engineering
Microsystems Engineering
Rochester, New York 14623
E-mail: wxz4550@rit.edu

Abstract. In this paper, we propose an optical switch based on a metal-insulator-metal plasmonic waveguide with Si$_3$N$_4$ core sandwiched between two gallium (Ga) metal layers. Combining the unique structural phase transition property of gallium, within a total length of only 400 nm, an extinction ratio as high as 7.68 dB can be achieved in the proposed nanoplasmonic structure. The phase transition may be achieved by changing the temperature of the waveguide or by external light excitation. © *2011 Society of Photo-Optical Instrumentation Engineers (SPIE)*. [DOI: 10.1117/1.3595868]

1 Introduction

Silicon-based photonic components and circuits are widely used in information processing and data storage. Optical switches and modulators, as essential elements in the circuits, have been studied intensely.[1,2] However, due to the relatively weak nonlinear optical properties of silicon, i.e., the weak dependence of refractive index and absorption coefficient on the free-carrier concentration,[3] these devices are only achieved by using very high power in large or nonplanar structures,[4–6] which make them not suitable for dense circuit component integration and hence limits their applications. A promising solution may be found in surface plasmon polaritons (SPPs), i.e., surface electromagnetic excitations coupled with collective electrons, which have intrigued considerable interest. Since SPPs exhibit extremely small guiding wavelengths and high field intensities along dielectric-metal interfaces, optical confinement can be scaled to deep subwavelength dimensions in plasmonic devices. A wide range of passive SPP-based circuit elements, which include waveguides,[7] couplers,[8] interferometers,[9,10] splitters,[11,12] reflectors,[13] wavelength demultiplexers,[14] and resonators,[15] have been proposed and successfully demonstrated. Furthermore, the strong confinement of the field to the interface renders the SPP propagation to be extremely sensitive to the minor changes of optical properties in the vicinity of dielectric-metal interface, which may be induced by the refractive index change of the dielectric materials or the metals. In this context, dynamic control of SPP propagation properties has been realized by using different approaches; most of them rely on the manipulation of the refractive index of the dielectric material adjacent to the metal surface by applying voltages[16–20] or illuminating pump light on the dielectric material.[21–24] In addition, plasmonic modulators based on quantum dots,[25] ferroelectric materials,[26] and liquid crystals[27] have been studied. Another example is a metal-oxide-silicon field effect plasmonic modulator, called "plasMOSter," which works by switching off the photonic mode when voltage is applied and therefore only supports plasmonic mode.[28] Strong modulation of the electromagnetic fields of SPPs is also achieved by implementing an

external magnet to control electrons of the ferromagnet in a gold-ferromagnet-gold structure.[29]

Recently, considerable interest arises in the nonlinear effect enhancement by structural phase transitions in polyvalent metals, for example, Ga, which has already shown to enable all optical switching at megawatt power levels.[30] Ga is a material known for its polymorphism.[31] The stable "ground-state" phase, α-gallium, is a highly anisotropic metal because molecular and metallic properties may coexist.[32] The phase transitions between α-gallium and metallic gallium will occur when the temperature is close to the melting temperature of α-gallium, which is very low as $29.8\,^\circ$C. The switching may be achieved by external optical excitation or just simply changing the temperature of the metal with the switching time approximately in the picosecond–microsecond range.[33] The significant difference in the optical properties of α-phase and metallic phase makes gallium a very suitable material for plasmonic modulators and switches. In 2004, Krasavin and Zheludev proposed an Au/Ga waveguide, which contains a 2.5-μm long gallium switching layer. Surface plasmon signals in the waveguide can be efficiently controlled by switching the structural phases of Ga, and a signal modulation depth exceeding 80% is observed in the proposed structure.[30]

2 Structure Design

Based on the previous work done by Krasavin and Zheludev,[30] in this paper we employ the unique phase transition property of gallium and focus on the signal light transmission through a simple Ga-Si$_3$N$_4$-Ga waveguide. We use the finite-difference time-domain (FDTD) method[34,35] to investigate the switching properties of the plasmonic waveguide. In the FDTD simulations, the experimental data for the frequency-dependent dielectric constants of Ga is directly used,[36,37] including both the real and imaginary parts for the three main crystalline axes (*a*-axis, *b*-axis, and *c*-axis) of α-gallium and the metallic gallium. The simulated structure is created as a simple coupler by placing a Ga-Si$_3$N$_4$-Ga plasmonic waveguide embedded between two identical dielectric (silicon) waveguides, as shown in Fig. 1(a). The silicon waveguides and the Ga-Si$_3$N$_4$-Ga waveguide are aligned along the light propagation direction. The two silicon waveguides are used to couple optical signals into and out of the Ga-Si$_3$N$_4$-Ga waveguide, respectively. Recent work shows
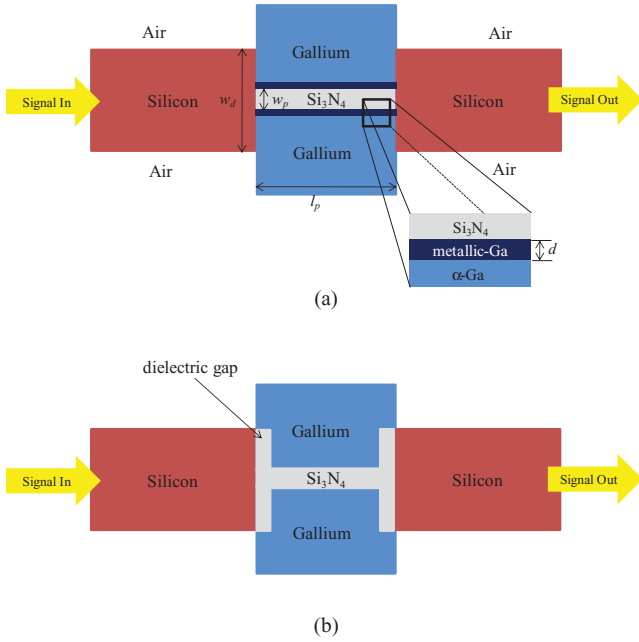
(a)

(b)

Fig. 1 (a) A Ga-Si$_3$N$_4$-Ga plasmonic waveguide embedded between two silicon dielectric waveguides, w_d: width of the dielectric waveguide, w_p: width of the dielectric core of the plasmonic waveguide, l_p: length of the plasmonic waveguide, d: thickness of the metallic gallium which is formed at Si$_3$N$_4$ and α-gallium interface. (b) Dielectric gaps are introduced at both ends of the plasmonic waveguide.

that high efficiency photonic-plasmonic-photonic coupling can be achieved through this configuration.[8] In order to calculate the power transmission of the Ga-Si$_3$N$_4$-Ga waveguide, a fundamental TM mode in the input silicon waveguide is excited by a mode source. The power fluxes are measured in both the input and output silicon waveguides. Since the center of attention describes the switching characteristics of the plasmonic waveguide, the parameter optimization of the whole structure to achieve high extinction ratios, as well as waveguide transmission, will be discussed later in the paper. We temporarily put the width of the silicon waveguides, w_d = 400 nm, the length of the Ga-Si$_3$N$_4$-Ga waveguide, l_p = 400 nm, and the width of dielectric core, w_p = 60 nm. Perfectly matched layers are used at all the boundaries of the simulation area to minimize the unnecessary reflection.[38] The spatial and temporal steps are set as $\Delta x = \Delta y = 2$ nm and $\Delta t = \Delta x/2c$[39] respectively, to ensure accurate results in the FDTD simulations and c is the speed of light in free space.

3 Two-Dimensional Simulation Results and Discussions

We investigate the different conditions when external optical excitation is applied and hence, the phase of gallium parts may completely switch between the ground phase, α-gallium, and the metallic phase. The simulations include all main crystalline orientations of α-gallium. First, we consider the different transmissions of the waveguide at a wavelength of 1550 nm. In the simulations, we assume that the gallium part is a homogeneous medium either in the α-phase or in the metallic phase. Figures 2(a) and 2(b) are the simulation results of the power distributions when the gallium is in the metallic phase and α-phase, CB (CB denotes the c-axis lying along the propagation direction and the b-axis lying along the
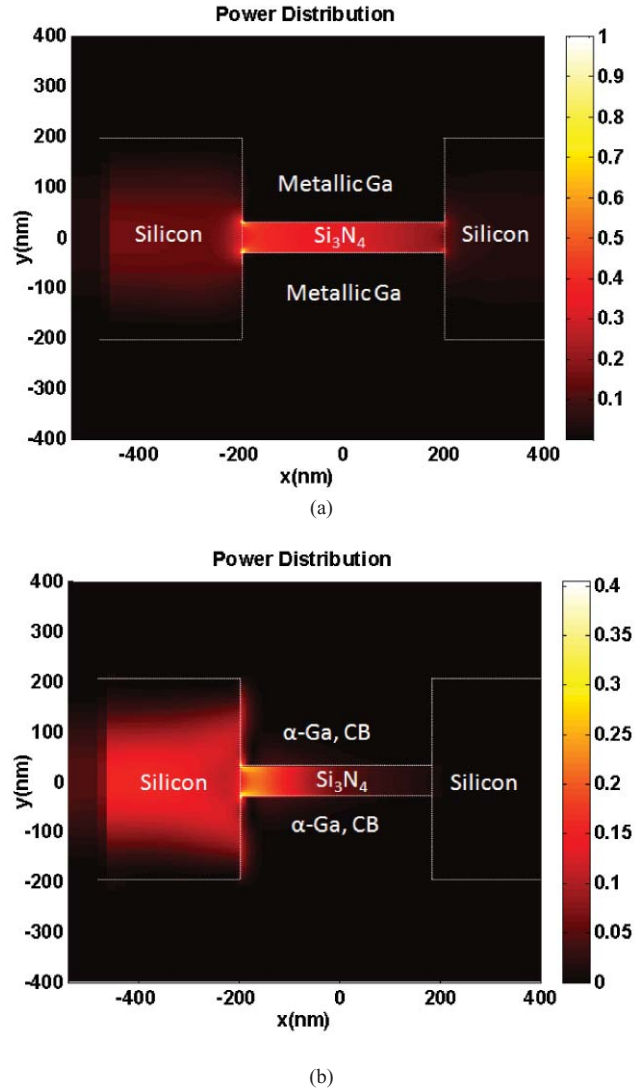

(a)

(b)

Fig. 2 (a) Simulation result of field distribution with metallic gallium. (b) Simulation result of field distribution with α-gallium, CB.

transverse direction which is perpendicular to the Ga-Si$_3$N$_4$ interface, similar notations will be used in other figures), respectively. For a better comparison, the two figures are normalized to the maximum value of the result with metallic gallium. Simulation results with the α-gallium in other crystalline directions showed similar power distributions as shown in Fig. 2(b). The power transmission decreases from 24.8% (with metallic gallium) to less than 5.77%, depending upon a specific crystalline direction, 1.36% for AB, 2.72% for AC, 4.4% for BA, 5.77% for BC, 1.62 for CA, and 1.06% for CB. Here, we define at a given wavelength,

$$\text{Extinction ratio (in dB)} = 10\log\left(\frac{T_{\text{metallic}}}{T_{\alpha\text{-max}}}\right), \qquad (1)$$

where $T_{\alpha\text{-max}}$ is the maximum transmission among those of the waveguide with α-gallium, and T_{metallic} is the transmission of the waveguide with metallic gallium at the same wavelength. Compared with the 2.5-μm long (the length of the gallium section, not including the lengths of the Au sections and the two 10 element coupling and decoupling gratings) structure in Ref. 26, an extinction ratio as high as 6.33 dB can
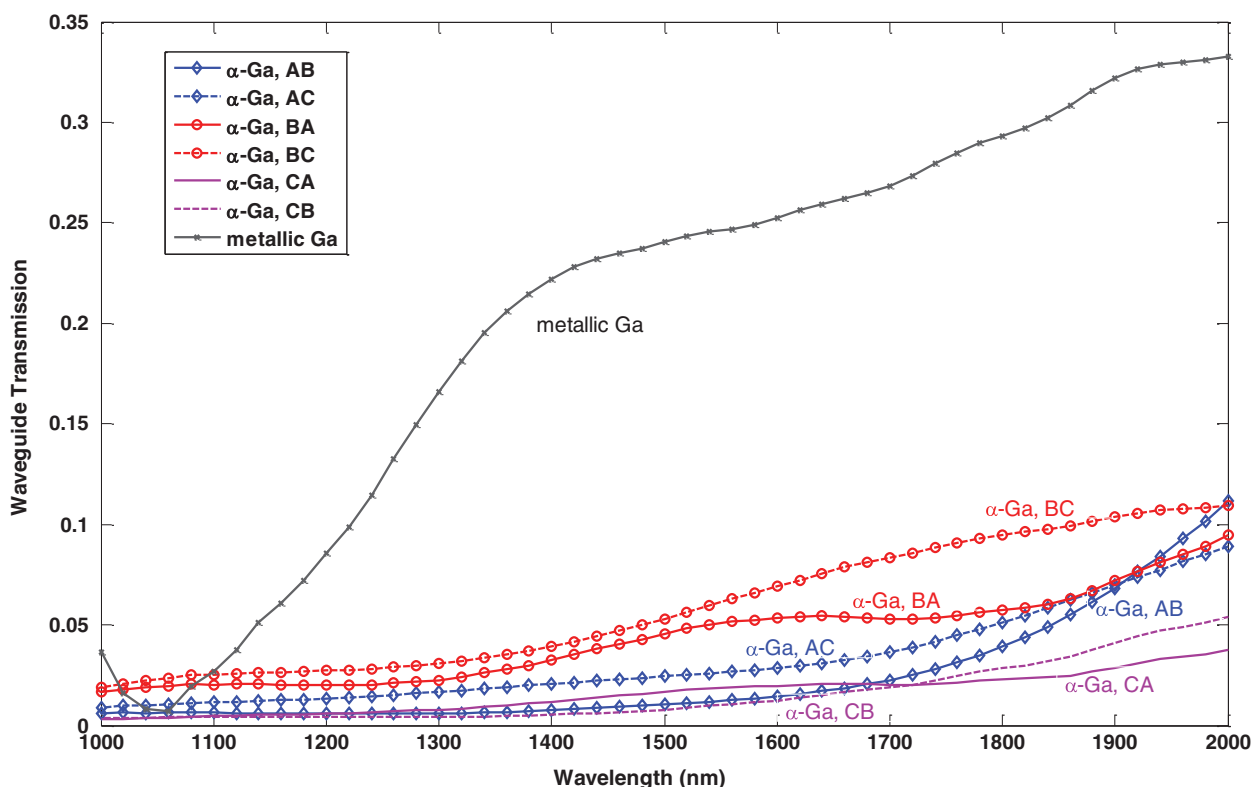
Fig. 3 Power transmission of the Ga-Si$_3$N$_4$-Ga plasmonic waveguide as a function of wavelength for different phases and crystalline directions of gallium.

be achieved in the simple Ga-Si$_3$N$_4$-Ga waveguide, with a total length of only 400 nm. This result is noticeable since the optical switch has been considered as a part of the integrated circuit, and the embedded structure is ready for fabrication. The detailed fabrication processes will be discussed with the three-dimensional (3D) structure, together in Sec. 4.

To further investigate the performance, we varied the working wavelengths of the optical switch from 1000 to 2000 nm in the simulations. Figure 3 shows the transmissions at different wavelengths of incident light for the same structure. The most important information obtained from the simulation results is that the structural phase of the gallium is the main factor to determine the transmission of the Ga-Si$_3$N$_4$-Ga waveguide. From Fig. 3, we find that as the wavelength increases, the transmission levels for all the cases increase, except for the transmission of the waveguide with metallic gallium decreases at a very narrow wavelength range (1000 to 1070 nm). We also note that an extinction ratio over 3 dB (not shown in Fig. 3) can be achieved at wavelengths approximately from 1160 to 2000 nm. The reason can be attributed to the following: when the structural phase of gallium changes, the changed refractive index of gallium will cause the propagation loss as well as the impedance change. By carefully examining Fig. 3, we found that at $\lambda = 1360$ nm, the extinction ratio reaches its maximum, which is 7.68 dB.

Transitions between different structural phases in a bulk material are not reversible and therefore would not be suitable for controlling light with light. However, this will become a dynamic coexistence of structural forms if the material is placed in a restrictive geometry. The simplest form of confinement is the formation of an interface with

another material.[32] The phase transition of gallium is a surface-mediated effect.[30] As shown in Fig. 1(a), we assume that a very thin layer of metallic gallium with thickness d develops at Si$_3$N$_4$ and α-gallium interface. The thickness of metallic gallium layer d will steadily increase with either temperature just below the gallium bulk melting point or incident light intensity.[30] We simulate the conditions as the thickness d of metallic gallium continuously increases. The transmissions of the waveguide for a series of incident wavelengths and the corresponding extinction ratios are shown in Figs. 4(a) and 4(b), respectively. In the simulations, a thin layer metallic gallium is sandwiched between Si$_3$N$_4$ and α-gallium, CB. The simulated structure and main geometric parameters are kept the same as the previous simulations. It is clearly seen that with the presence of tens of nanometers thick metallic gallium, the transmissions of the waveguide, as well as the extinction ratios, increase rapidly. This may be due to that only the metal in the vicinity of the metal-dielectric interface will be involved in the switching processes, since the field decays exponentially inside the metal at the interface. As shown in Fig. 4(b), at $\lambda = 1550$ nm, with a 40-nm thick metallic gallium layer, the extinction ratio reaches around 9.98 dB and the transmission increases to 10 times of its original value [see Fig. 4(a)].

The plasmonic waveguide with metallic gallium represents an "on" state while with α-gallium represents an "off" state. The transmission of the waveguide with metallic gallium can be improved by choosing the optimal geometric parameters of the waveguide or simply introducing dielectric gaps to the structure, as shown in Fig. 1(b). Those gaps may function like "funnels" to gather more SPPs to the dielectric
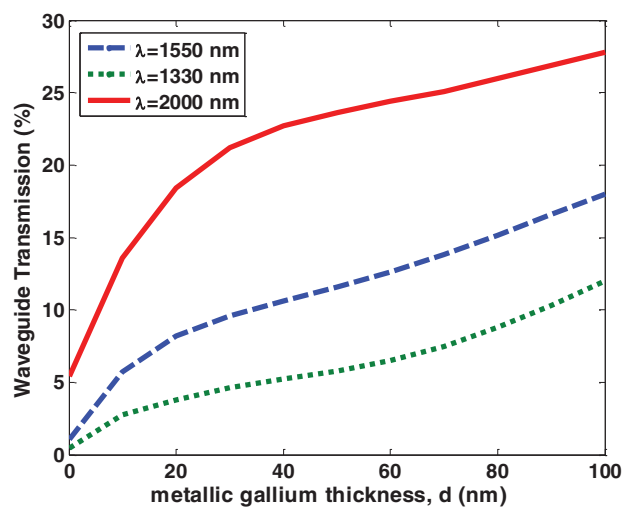
(a)
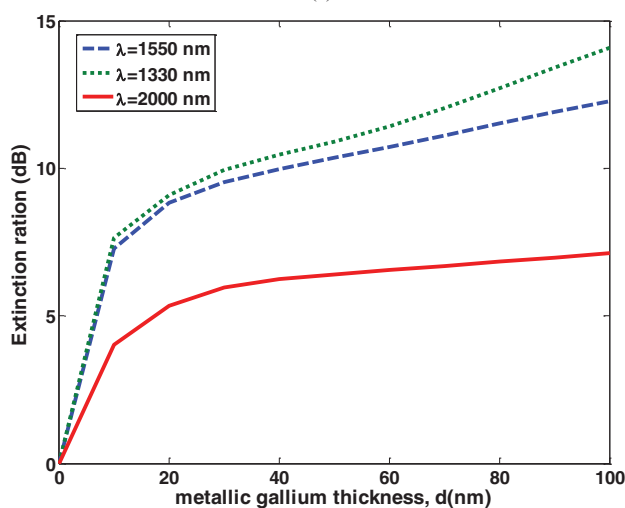
(b)

Fig. 4 (a) Power transmissions as a function of the depth *d* of metallic gallium thin film. (b) Extinction ratios of the Ga-Si$_4$N$_4$-Ga plasmonic waveguide as a function of *d*.

Fig. 5 (a) Starting the fabrication process on an SOI wafer. (b) Defining the input and output Si waveguide**s.** (c) Deposition of Si3N4 film as the core of the plasmonic waveguide. (d) Deposition of gallium film.

core of the waveguide.[12] With two 40-nm wide gaps placed at both ends of the plasmonic waveguide, at an incident wavelength of 1550 nm, the transmission of the waveguide with metallic gallium is improved to 30.3%, while the extinction ratio is approximate 7.05 dB. Other parameters (e.g., the width of Si$_3$N$_4$ core, w_p), can also be optimized to increase the power transmission. From simulation results, with increased core thickness w_p, the transmission of the waveguide will increase as well. For example, when $w_p = 90$ nm, transmission of the waveguide with metallic gallium increases to 39.7% at $\lambda = 1550$ nm. The whole structure exhibits Fabry–Pérot effect as the length of the plasmonic waveguide changes,[8] when the length of the Ga-Si$_3$N$_4$-Ga waveguide is 140 nm, transmission with metallic gallium is around 40.7%, and the extinction ratio is approximately 4.25 dB.

4 3D Implementation and Fabrication Steps

Until now, an efficient two-dimensional (2D) optical switch has been successfully demonstrated. Here, we propose a possible 3D implementation of the optical switch.
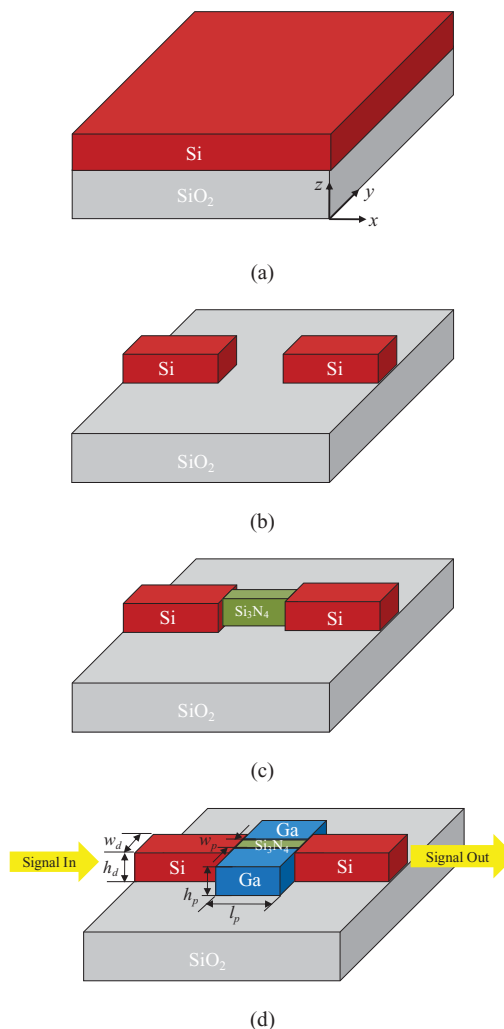
Figures 5(a)–5(d) illustrates the main fabrication steps of the optical switch. First, the input and output silicon waveguides will be fabricated on a silicon-on-insulator (SOI) wafer. In the second step, the dielectric core of the plasmonic waveguide, silicon nitride, will be deposited between the two silicon waveguides by a method named hot-wires chemical vapor deposition.[40] With NH$_3$/SiH$_4$ ratios between 40 and 70, and at low substrate temperature of 100°C or 250°C, dense films (2.56 to 2.74 g/cm^3) and refractive index between 1.93 and 2.08 can be obtained.[40] The following lithography and etch steps will pattern the dielectric core. Good alignment is required to make the dielectric core be in alignment with the input/output silicon waveguides in the *y*-axis. In the third step, a high quality gallium film will be deposited on the substrate from Ga targets using a *Q*-switched mode-locked Nd:YAG laser ($\lambda = 1.064~\mu$m; $\tau_{\text{FWHM}} = 60$ ps).[41] It has been reported that gallium nanoparticles with a relatively narrow size could be formed on the substrate if it was illuminated by very low intensity laser light.[42,43] The gallium film will re-solidify to α phase after the melting process.[41]

To characterize the optical switch in a 3D configuration and compare the extinction ratios with the 2D switch, the
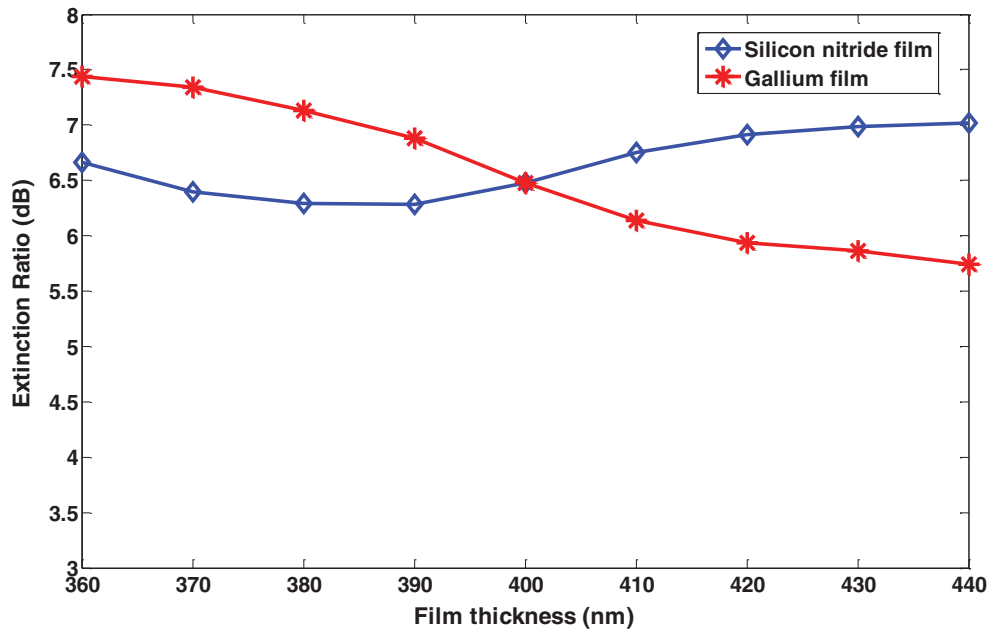
Fig. 6 Extinction ratio as a function of thickness of silicon nitride or gallium film.

dimensions of the optical switch is similar to those in 2D simulations. The cross section of the Si waveguides in the y-z plane is assumed to be square, where the height of the Si waveguides h_d equals the width w_d to be 400 nm. The height of the plasmonic waveguide h_p is identical as h_d. The length l_p and the width w_p are set as $l_p = 400$ nm and $w_p = 60$ nm, respectively. In the 3D numerical simulations, the gallium is either in the metallic phase or in the α-phase. The same notation of gallium in the α-phase is used, for example, CB represents c-axis lying in the light propagation direction, x-axis, b-axis lying in the z-axis, and a-axis lying in the y-axis. A mode with the main component of E in the y direction is excited in the input silicon waveguide. The power transmission measured at the output silicon waveguide is as follows: 31.1% for metallic gallium, 1.2% for AB, 2.95% for AC, 4.3% for BA, 7.0% for BC, 1.34% for CA, and 1.0% for CB. The extinction ratio using Eq. (1) is calculated as 6.48 dB, which is consistent with that of the 2D switch, 6.33 dB.

Recently, experimental demonstrations of plasmonic waveguide[44] and coupler[45] have been reported. Different from our proposed structure, the core material of the fabricated waveguides is air. One challenge of the fabrication process for our structure is the conformality of each deposited film. In order to show how the thicknesses of the silicon nitride or the gallium film will impact the extinction ratio, we performed a series of simulations with the conditions that either the silicon nitride or the gallium film was not at the target thickness, which is 400 nm. Figure 6 shows the extinction ratio as a function of the thickness of silicon nitride or gallium. For simplicity, in each simulation, only one film (silicon nitride or gallium) thickness varies, while the other one has a thickness of 400 nm. The range of thickness variation is 400 ± 40 nm. From the results, it is seen that gallium film thickness is more critical, since $\pm 10\%$ thickness variation will cause a maximum 15% extinction ratio change, while with the same thickness variation, silicon nitride will only bring an 8.4% change in extinction ratio.

5 Conclusions

Recently, all-optic switching has also been reported in metal-insulator-metal waveguides with Kerr nonlinear defects.[46,47] Compared with the plasmonic waveguides proposed in those papers, the switching mechanism of our Ga-Si₃N₄-Ga waveguide mainly depends on the waveguide material (gallium) property, not by introducing an additional nonlinear medium. Hence, our proposed structure is much simpler and easier to fabricate.

To summarize, we have investigated the potential switching properties of a simple Ga-Si₃N₄-Ga plasmonic waveguide. With a length of only 400 nm, an extinction ratio as 7.68 dB can be achieved in the proposed structure. Since the phase transition of gallium is a surface-mediated effect, we also show that with tens of nanometers thick metallic gallium sandwiched between Si₃N₄ and α-gallium, the power transmission level will increase greatly. Further study on the parameter optimization confirms that the transmission of the waveguide can be improved to 40.7%, while the extinction ratio is still kept over 4.25 dB.

References

1. S. R. Friber, Y. Silberberg, M. K. Oliver, M. J. Andrejco, and M. A. Saifi, "Ultrafast all-optical switching in a dual-core fiber nonlinear coupler," *Appl. Phys. Lett.* **51**, 1135–1137 (1987).
2. V. R. Almeida, C. A. Barrios, R. R. Panepucci, and M. Lipson, "All-optical control of light on a silicon chip," *Nature* **431**, 1081–1084 (2004).
3. R. A. Soref and B. R. Bennett, "Electrooptical effects in silicon," *IEEE J. Quant. Electron.* **QE-23**, 123–129 (1987).

4. G. Cocorullo, F. G. Della Corte, R. De Rosa, I. Rendina, A. Rubino, and E. Terzini, "Fast infrared light modulation in a-Si:H micro-devices for fiber-to-the-home applications," *J. Non-Cryst. Solids* **266–269**, 1247–1251 (2000).

5. H. K. Tsang, C. S. Wong, T. K. Liang, I. E. Day, S. W. Roberts, A. Harpin, J. DrakeH, and M. Asghari, "Optical dispersion, two-photon absorption, and self-phase modulation in silicon waveguides at 1.5 mm wavelength," *Appl. Phys. Lett.* **80**, 416–418 (2002).

6. A. Hache and M. Bourgeois, "Ultrafast all-optical switching in a silicon-based photonic crystal," *Appl. Phys. Lett.* **77**, 4089–4091 (2000).

7. R. Zia, M. D. Selker, P. B. Catrysse, and M. L. Brongersma, "Geometries and materials for subwavelength surface plasmon modes," *J. Opt. Soc. Am. A* **21**, 2442–2446 (2004).

8. G. Veronis and S. Fan. "Theoretical investigation of compact couplers between dielectric slab waveguides and two-dimensional metal-dielectric-metal plasmonic waveguides," *Opt. Express* **15**(3), 1211–1221 (2007).

9. H. F. Schouten, N. Kuzmin, G. Dubois, T. D. Visser, G. Gbur, P. F. A. Alkemade, H. Blok, G. W. Hooft, D. Lenstra, and E. R. Eliel, "Plasmon-assisted two-slit transmission: young's experiment revisited," *Phys. Rev. Lett.* **94**, 053901 (2005).

10. R. Zia and M. L. Brongersma, "Surface plasmon polariton analogue to Young's double-slit experiment," *Nat. Nanotechnol.* **2**, 426–429 (2007).

11. S. I. Bozhevolnyi, V. S. Volkov, E. Devaux, J. Y. Laluet, and T. W. Ebbesen, "Channel plasmon subwavelength waveguide components including interferometers and ring resonators," *Nature* **440**, 508–511 (2006).

12. R. A. Wahsheh, Z. Lu, and M. A. G. Abushagur, "Nanoplasmonic couplers and splitters," *Opt. Express* **17**, 19033 (2009).

13. Y. Gong, L. Wang, X. Hu, X. Li, and X. Liu, "Broad-bandgap and low-sidelobe surface plasmon polariton reflector with Bragg-grating-based MIM waveguide," *Opt. Express* **17**, 13727–13736 (2009).

14. G. Wang, H. Lu, X. Liu, D. Mao, and L. Duan, "Tunable multi-channel wavelength demultiplexer based on MIM plasmonic nanodisk resonators at telecommunication regime," *Opt. Express* **19**, 3513–3518 (2011).

15. A. Hosseini and Y. Massoud, "Nanoscale surface Plasmon based resonator using rectangular geometry," *Appl. Phy. Lett.* **90**, 181102 (2007).

16. W. S. Cai, J. S. White, and M. L. Brongersma, "Compact, high-speed, and power-efficient electrooptic plasmonic modulators," *Nano. Lett.* **9**, 4403–4411 (2009).

17. T. Nikolajsen and K. Leosson, "Surface plasmon polariton based modulators and switches operating at telecom wavelengths," *Appl. Phys. Lett.* **85**, 5833–5835 (2004).

18. M. J. Dicken, L. A. Sweatlock, D. Pacifici, H. J. Lezec, K. Bhattacharya, and H. A. Atwater, "Electrooptic modulation in thin film barium titanate plasmonic interferometers," *Nano Lett.* **8**, 4048–4052 (2008).

19. Z. Wu, R. L. Nelson, J. W. Haus, and Q. W. Zhan, "Plasmonic electro-optic modulator design using a resonant metal grating," *Opt. Lett.* **33**(6), 55–553 (2008).

20. C. Jung, S. Yee, and K. Kuhn, "Electro-optic polymer light modulator based on surface Plasmon resonance," *Appl. Optics* **34**(6), 946–949 (1995).

21. J. Dintinger, I. Robel, P. V. Kamat, C. Genet, and T. W. Ebbesen, "Terahertz all-optical molecule-plasmon modulation," *Adv. Mater.* **18**, 1645–1648 (2006).

22. R. A. Pala, K. T. Shimizu, N. A. Melosh, and M. L. Brongersma, "A nonvolatile plasmonic switch employing photochromic molecules," *Nano Lett.* **8**(5), 1506–1510 (2008).

23. K. Sasaki and T. Nagamura, "Ultrafast all-optical switch using complex refractive index changes of thin films containing photochromic dye," *Appl Phys. Lett.* **71**(4), 434–436 (1997).

24. C. Min and G. Veronis, "Absorption switches in metal-dielectric-metal plasmonic waveguides," *Opt. Express* **17**, 10757–10766 (2009).

25. D. Pacifici, H. J. Lezec, and H. A. Atwater, "All-optical modulation by plasmonic excitation of CdSe quantum dots," *Nat. Photonics* **1**, 402–406 (2007).

26. S. W. Liu and M. Xiao, "Electro-optic switch in ferroelectric thin films mediated by surface plasmons," *Appl. Phys Lett* **88**, 143512 (2006).

27. P. R. Evans, G. A. Wurtz, W. R. Hendren, R. Atkinson, W. Dickson, A. V. Zayats, and R. J. Pollard, "Electrically switches nonreciprocal transmission of plasmonic nanorods with liquid crystal," *Appl. Phys. Lett.* **91**, 043101 (2007).

28. J. A. Dionne, K. Diest, L. A. Sweatlock, and H. A. Atwater, "Plas-MOStor: A metal-oxide-si field effect plasmonic modulator," *Nano Lett.* **9**(2), 897–902 (2009).

29. V. V. Temnov, G. Armelles, U. Woggon, D. Guzatov, A. Cebollada, A. Garcia-Martin, J. M. Garcia-Martin, T. Thomay, A. Leitenstorfer, and R. Bratschitsch, "Active magneto-plasmonics in hybrid metal–ferromagnet structures," *Nature Photon.* **4**, 107–111 (2010).

30. A. V. Krasavin and N. I. Zheludev, "Active plasmonics: controlling signals in Au/Ga waveguide using nanoscale structural transformations," *Appl. Phys. Lett.* **84**, 1416–1418 (2004).

31. L. Bosio, "Crystal structures of Ga(II) and Ga(III)," *J. Chem. Phys.* **68**, 1211–1223 (1978).

32. N. Zheludev, "Nonlinear optics on the nanoscale," *Contemp. Phys.* **43**, 365–377 (2002).

33. V. Albanis, S. Dhanjal, V. I. Emelyanov, V. A. Fedotov, K. F. MacDonald, P. Petropoulos, D. J. Richardson, and N. I. Zheludev, "Nanosecond dynamics of a gallium mirror's light-induced reflectivity change," *Phys. Rev. B* **63**, 165207 (2001).

34. A. Taflove and S. C. Hagness, "Computational Electrodynamics: The Finite-Difference Time-Domain Method," *Artech House*, Norwood (2005).

35. K. S. Yee, "Numerical solution of initial boundary value problems involving Maxwell's equations," *IEEE Trans. Antennas Propag.* **14**, 302–307 (1966).

36. R. Kofman, P. Cheyssac, and J. Richard, "Optical properties of Ga monocrystal in the 0.3–5-ev range," *Phys. Rev. B* **16**, 5216–5244 (1977).

37. E. D. Palik, ed., *Handbook of Optical Constants of Solids* Academic, New York (1984).

38. J. Jin, "The Finite Element Method" in *Electromagnetics*, (Wiley, New York, 2002).

39. Y. Shen and G. Wang, "Optical bistability in metal gap waveguide nanocavities," *Opt. Express* **16**, 8421–8426 (2008).

40. P. Alpuim, L. M. Gonçalves, E. S. Marins, T. M. R. Viseu, S. Ferdov, and J. E. Bourée, "Deposition of silicon nitride thin films by hot-wire CVD at 100 ºC and 250 ºC", *Thin Solid Films* **517**, 3503–3506 (2009).

41. A. V. Rode, M. Samoc, B. Luther-Davies, E. G. Gamaly, K. F. MacDonald, and N. I. Zheludev, "Dynamics of light-induced reflectivity switching in gallium films deposited on silica by pulsed laser ablation," *Opt. Lett.* **26**, 441–443 (2001).

42. K. F. MacDonald, V. A. Fedotov, S. Pochon, K. J. Ross, G. C. Stevens, N. I. Zheludev, W. S. Brocklesby, and V. I. Emel'yanov, "Optical control of gallium nanoparticle growth," *Appl. Phys. Lett.* **80**, 1643–1645 (2002).

43. V. A. Fedotov, K. F. MacDonald, N. I. Zheludev, and V. I. Emel'yanov, "Light-controlled growth of gallium nanoparticles," *J. Appl. Phys.* **93**, 3540–3544 (2003).

44. J. Tian, S. Yu, W. Yan, and M. Qiu, "Broadband high-efficiency surface-plasmon-polariton coupler with silicon-metal interface," *Appl. Phy. Lett.* **95**, 013504 (2009).

45. Z. Han, A. Elezzabi, and V. Van, "Experimental realization of subwavelength plasmonic slot waveguides on a silicon platform," *Opt. Lett.* **35**, 502–504 (2010).

46. H. Lu, X. Liu, L. Wang, Y. Gong, and D. Mao, "Ultrafast all-optical switching in nanoplasmonic waveguide with Kerr nonlinear resonator," *Opt. Express* **19**, 2910–2915 (2011).

47. H. Lu, X. Liu, Y. Gong, D. Mao, and L. Wang, "Optical bistability in metal-insulator-metal plasmonic Bragg waveguides with Kerr nonlinear defects," *Appl. Opt.* **50**, 1307–1311 (2011).

Wangshi Zhao received her BS degree in information science and electrical engineering from Zhejiang University. Currently, she is a PhD student of microsystems engineering, Rochester Institute of Technology. Her research area includes nano-plasmonics and metamaterials.

Zhaolin Lu is currently an assistant professor in the Department of Microsystems Engineering, Rochester Institute of Technology, where he established the Nanoplasmonics and Metamaterials Laboratory. The focus of this laboratory is on both the theoretical and experimental aspects of metamaterials, photonic crystals, active and passive nanophotonic elements and their integration into opto-electronic subsystems. His research interests include passive and active nanoplasmonic devices, photonic crystal devices, and optical waveguides for application in next-generation opto-electronic systems, 3D metamaterials and applications, and 3D negative refraction imaging.